

Mesons in a Poincare Covariant Bethe–Salpeter Approach

R. Alkofer, P. Watson, and H. Weigel*

Institute for Theoretical Physics, Tübingen University

D-72076 Tübingen, Germany

(October 26, 2018)

hep-ph/0202053

UNITU-HEP-4/2002

Abstract

We develop a covariant approach to describe the low-lying scalar, pseudoscalar, vector and axialvector mesons as quark–antiquark bound states. This approach is based on an effective interaction modeling of the non-perturbative structure of the gluon propagator that enters the quark Schwinger–Dyson and meson Bethe–Salpeter equations. We consistently treat these integral equations by precisely implementing the quark propagator functions that solve the Schwinger–Dyson equations into the Bethe–Salpeter equations in the relevant kinematical region. We extract the meson masses and compute the pion and kaon decay constants. We obtain a quantitatively correct description for pions, kaons and vector mesons while the calculated spectra of scalar and axialvector mesons suggest that their structure is more complex than being quark–antiquark bound states.

PACS: 14.40.-n, 11.10.St, 12.38.Lg

*Heisenberg–Fellow

I. INTRODUCTION

Recently, the scalar mesons have attracted a lot of interest as the reanalysis of the pseudoscalar meson scattering data indicated the existence of a flavor $SU(3)$ nonet in this channel [1]. It is therefore desirable to gain deeper understanding of the constituent structure of the scalar mesons together with a comprehensive description of the meson states in the other spin–parity channels. The ultimate goal would be to understand all low–lying meson states and resonances as non–perturbative bound states in Quantum Chromo Dynamics (QCD).

A relativistic framework for analyzing mesons as composite objects is provided by the Bethe–Salpeter equations that extract poles in the quark–antiquark scattering kernel [2]. The attraction needed to bind quarks and antiquarks emerges from dressed multiple gluon exchange. Thus the essential ingredients to these equations are the quark and gluon propagators as well as the quark–gluon vertex. In addition, these n -point Green’s functions are related by their Schwinger–Dyson equations which are part of an infinite tower of non–linear integral equations. There has been some progress in the understanding of the infrared behavior of the gluon propagator from recent Yang–Mills lattice calculations [3] as well as from studies of the coupled system of gluon and ghost Schwinger–Dyson equations [2,4]. Nevertheless, for phenomenological applications the frequently adopted strategy is to model the gluon propagator as well as the quark–gluon vertex and consistently derive the quark propagator from its Schwinger–Dyson equation because it facilitates the continuation to complex Euclidean momenta.

These types of calculations have a long history, for reviews see Refs. [2,5]. Early versions adopted pointlike gluon propagators in coordinate space that eventually lead to Nambu–Jona–Lasinio (NJL) type models [6,7], pointlike propagators in momentum space were also considered [8]. These models are particularly simple because either solving the Schwinger–Dyson equation yields a free quark propagator or the Bethe–Salpeter integral equations reduce to algebraic equations. The main target particularly of the NJL–model studies have been the pseudoscalar mesons. It turned out that they can be adequately described once the important feature of dynamical chiral symmetry breaking is incorporated, *i.e.* the interaction is strong enough so that the resulting quark propagator signals a non–vanishing quark condensate reflected by a non–zero constituent quark mass. Then the pseudoscalar mesons can be understood as the *would-be* Goldstone bosons of chiral symmetry breaking. However, as the Bethe–Salpeter equations involve the dressed (constituent) quark propagators, binding can only be achieved kinematically and meson states with masses larger than twice the constituent quark mass cannot be described consistently. For that reason, model gluon propagators have been developed that yield quark propagators without poles for real momenta as an attempt to include the confinement phenomena [9,10]. Again these studies focused on pseudoscalar mesons [11,12] while a comprehensive investigation for the scalar, pseudoscalar, vector and axialvector mesons has not been carried out so far. Other studies [9,10] made contact with perturbative QCD by considering a model gluon propagator that matches the pertinent anomalous dimension. This contribution has negligible effect on the meson properties, but its inclusion makes cumbersome the extraction of the solutions to the Schwinger–Dyson equations for the large time–like momenta that enter the Bethe–Salpeter equations with meson states other than the pseudoscalars. We consider this attempt interesting, but as we do not want to focus on the ultraviolet properties of mesons here, we

regard it an unnecessary technical complication. Therefore we focus rather on establishing a model as simple as possible that we consider a pertinent starting point to study the structure and properties of low-lying mesons in a relativistic framework. Our model interaction is parameterized in form of a non-trivial gluon propagator that contains sufficient strength to cause dynamical chiral symmetry breaking. For technical reasons it turns out that a Gaussian shape function for the propagator in momentum space is most suitable. Essentially we consider this model propagator as an effective interaction that relativistically describes the binding of quarks and antiquarks to mesons. Furthermore, we take the quark-gluon vertex function to be the tree level one since this procedure provides a framework that is consistent with chiral symmetry when the ladder approximation for the Bethe-Salpeter equation is employed [2,5]. For approaches going beyond ladder approximation see e.g. Ref. [13].

This paper is organized as follows. In Section II we will introduce the effective interaction and solve the Schwinger-Dyson equation for the quarks. We will put particular emphasis on the analytic continuation of the resulting quark propagator to time-like momenta that enter the Bethe-Salpeter equations. We will discuss the structure of the Bethe-Salpeter equations and present the solutions in Section III. In Section IV we will present the numerical results in the sector of the three light quarks (up, down and strange) and compare them to the empirical data. In Section V we will conclude and suggest a possible extension of the current approach in particular with regard to the possibility that the scalar meson might have to be considered as two-quark – two-antiquark bound states [1,14]. We devote an appendix to discuss the numerical stability of our results.

II. THE QUARK SCHWINGER-DYSON EQUATION

The purpose of this section is twofold. First we will explain our model gluon propagator whose dressing parameterizes the effective interaction and then solve the corresponding Schwinger-Dyson equation for the quark propagator.

As already discussed in the introduction we take a Gaussian form for dressing the model gluon propagator. This follows the work of Ref. [10] with the exception that we omit the logarithmic tail that matches perturbative QCD because we are not interested in the ultraviolet properties of mesons. We therefore write,

$$g^2 G_{\mu\nu}^{ab}(q) = 4\pi^2 D \delta^{ab} t_{\mu\nu}(q) \frac{q^2}{\omega^2} \exp\left(-\frac{q^2}{\omega^2}\right) \quad (1)$$

where μ, ν are Lorentz indices, $t_{\mu\nu}(q)$ is the transverse momentum projector and a, b label color. While the prefactors in eq. (1) are chosen to make subsequent equations more concise, D and ω are dimensionful parameters that we will determine from fitting empirical data. The coefficient D sets the strength of the interaction and ω is the value at which the scalar function in the parameterization is maximal. Hence ω sets the interaction scale. The dressed gluon propagator (1) is supposed to represent a sensible hadron model and hence one can envisage that ω will have a value of several hundred MeV.

We interpret the effective interaction (1) as the propagator (in Landau gauge) of a gluon that gets absorbed and emitted by the quarks that eventually get bound to form mesons. To completely define the interaction, we need to parameterize the quark-gluon coupling.

To establish chiral symmetry we apply the rainbow–ladder approximation to the system of Schwinger–Dyson and Bethe–Salpeter equations. This implies that the quark–gluon coupling is given by the tree level interaction vertex, $ig\gamma_\mu\frac{\lambda^a}{2}$, where λ^a is a Gell–Mann matrix acting in color space. Note, that we have already included the coupling constant g in the definition of the effective interaction (1).

Then the Schwinger–Dyson equation for the (inverse) quark propagator becomes ($\int d^4k/(2\pi)^4$)

$$S^{-1}(p) = i\not{p} + m_0 + \int d^4k \gamma_\mu S(k) \gamma_\nu g^2 \frac{\lambda^a \lambda^b}{2} G_{\mu\nu}^{ab}(k-p) \quad (2)$$

where m_0 is the current mass of the considered quark. This contribution represents the only explicit distinction between quarks of different flavors. Of course, its effects will implicitly propagate through the whole calculation. However, for notational simplicity we will continue to suppress flavor labels. A suitable parameterization of the quark propagator is inspired by the form of a free fermion propagator

$$S(p) = \left[\frac{1}{i\not{p}A(p^2) + B(p^2)} \right]. \quad (3)$$

In solving the Schwinger–Dyson equation (2) we have to find the scalar functions $A(p^2)$ and $B(p^2)$. It is also very instructive to define a mass function via $M(p^2) = B(p^2)/A(p^2)$. In particular $M(p^2 = 0)$ plays the role of a constituent quark mass and a large value thereof signals dynamical chiral symmetry breaking.

As usual we work in Euclidean space with Hermitian Dirac matrices¹ that obey $\{\gamma_\mu, \gamma_\nu\} = 2\delta_{\mu\nu}$ and $\gamma_5 = -\gamma_1\gamma_2\gamma_3\gamma_4$. Inserting the effective interaction (1) and performing the standard trace algebra, we then deduce the following coupled equations for the propagator functions

$$A(x) = 1 + \frac{D}{\omega^2} \int_0^\infty \frac{dy y A(y)}{(yA^2(y) + B^2(y))} \\ \times \frac{2}{\pi} \int_{-1}^1 dz \sqrt{1-z^2} \left[-\frac{2}{3}y + \left(1 + \frac{y}{x}\right) \sqrt{xy} z - \frac{4}{3}yz^2 \right] \exp \left\{ -\frac{x+y-2\sqrt{xy}z}{\omega^2} \right\}, \quad (4)$$

$$B(x) = m_0 + \frac{D}{\omega^2} \int_0^\infty \frac{dy y B(y)}{(yA^2(y) + B^2(y))} \\ \times \frac{2}{\pi} \int_{-1}^1 dz \sqrt{1-z^2} [x+y-2\sqrt{xy}z] \exp \left\{ -\frac{x+y-2\sqrt{xy}z}{\omega^2} \right\}, \quad (5)$$

where the four dimensional integral measure has been expanded such that $x = p^2, y = k^2$ and $z = p \cdot k / \sqrt{p^2 k^2}$.

In a first step we solve eqs. (4) and (5) for spacelike momenta, *i.e.* for real positive x . Then we observe that the integrals on the *RHS* of these equations only involve the propagator functions at real arguments y and we can use them to numerically compute the

¹This can be related to the standard Minkowski space Dirac matrices via $\gamma_4 = \gamma_0^M, \gamma_j = -i\gamma_j^M$.

propagator functions for *arbitrary complex* x . At first sight, it appears that $A(x)$ and $B(x)$ could not be consistently continued because the cut along the negative x -axis (associated with \sqrt{x}) would yield different results when continuing in the upper or the lower half-plane and it would be impossible to resolve the ambiguity in $\sqrt{x} \rightarrow \pm i\sqrt{\xi}$ when continuing $x \rightarrow -\xi$. Fortunately, this is not an obstacle. By expanding the exponential functions in eqs. (4) and (5) it becomes obvious that all terms that contain \sqrt{x} are odd in z and thus vanish when integrating over this angular variable. Thus we are free to choose either of the two signs above. For definiteness we work in the upper half-plane with $\sqrt{x} \rightarrow i\sqrt{\xi}$ along the negative half-line.

The observation that it is sufficient to know the propagator functions along the real positive axis to compute them for all complex arguments of interest is a major point of this present study. It is an especially important issue to the study of the Bethe–Salpeter equation, since the quark propagator must be sampled in the complex plane of Euclidean momenta. In other words, the quark functions are calculated at precisely the momenta for which they are used, with no fitting functions, interpolation or extrapolation. However, in order to do so numerically, the quark propagator functions must be known very accurately along the real positive axis. This is achieved by noting that in eqs. (4) and (5) the angular (z) integrals can be done analytically for real and positive x . This property of the angular integrals is a particular feature of the Gaussian dressing function (1). The resulting equations read

$$\begin{aligned}
A(x) &= 1 + D \int_0^\infty \frac{dy y A(y)}{(yA^2(y) + B^2(y))} \exp\left\{-\frac{x+y}{\omega^2}\right\} \\
&\quad \times \left\{ \left(1 + \frac{y}{x} + 2\frac{\omega^2}{x}\right) I_2\left(\frac{2\sqrt{xy}}{\omega^2}\right) - 2\frac{\sqrt{y}}{\sqrt{x}} I_1\left(\frac{2\sqrt{xy}}{\omega^2}\right) \right\}, \\
B(x) &= m_0 + D \int_0^\infty \frac{dy y B(y)}{(yA^2(y) + B^2(y))} \exp\left\{-\frac{x+y}{\omega^2}\right\} \\
&\quad \times \left\{ \left(\frac{\sqrt{y}}{\sqrt{x}} + \frac{\sqrt{x}}{\sqrt{y}}\right) I_1\left(\frac{2\sqrt{xy}}{\omega^2}\right) - 2I_2\left(\frac{2\sqrt{xy}}{\omega^2}\right) \right\}, \tag{6}
\end{aligned}$$

where I_n are modified Bessel functions. These equations are one-dimensional coupled non-linear integral equations which can be straightforwardly solved numerically with a high degree of precision. The solutions for real (Euclidean) momenta are subsequently substituted into eqs. (4) and (5) to yield the propagator functions for complex momenta.

III. THE BETHE-SALPETER EQUATION

Having obtained the quark propagators in the complex plane from the Schwinger–Dyson equations we have collected all ingredients for the Bethe–Salpeter integral equations. They will ultimately yield the quark meson vertex functions, Γ , that describe mesons as bound quark–antiquark pairs. Strictly speaking, the Bethe–Salpeter equation is an eigenvalue problem, valid only at the resonance pole $P^2 = -M^2$, where M is the mass of the resonance. It is derived from considering the four-point quark Green’s function that involves exchanges of resonance mesons. Such an exchange is characterized by a pole in that four-point function, and the homogeneous Bethe–Salpeter equation below (7) determines the position of that pole. All other regular terms in the vicinity of this pole are neglected. Demanding

furthermore that the residue of this pole is unity yields the normalization condition (14) for the vertex functions.

A. Bethe–Salpeter vertex functions

The vertex functions resulting from the Bethe–Salpeter equation are characterized by three momenta out of which only two are linearly independent due to momentum conservation at the vertex. If we denote the meson momentum P and the momentum of the incoming quark $p + \xi P$ then the momentum of the outgoing quark (= incoming antiquark) is $p + (\xi - 1)P$. This suggests to label the vertex functions by p and P : $\Gamma(p, P)$. We have also introduced the arbitrary momentum partition parameter $\xi \in [0, 1]$. Due to strict relativistic covariance the results for physical observables do not depend on ξ . Unfortunately we will have to assume approximations within the full numerical computation (see Section 4) that violate covariance to some extent. We will study the ξ –dependence of our results and verify that within a wide range ξ –independence is maintained, see Appendix A. This will represent an *a posteriori* validation for the relativistic covariance of our computations.

We now turn to the main target of our studies, the Bethe–Salpeter integral equations for the vertex function $\Gamma(p, P)$ in ladder approximation [2,5,15]:

$$\Gamma(p; P) = -\frac{4}{3} \int \bar{d}^4k [\gamma_\nu S(k + \xi P) \Gamma(k; P) S(k + (\xi - 1)P) \gamma_\mu] g^2 G_{\mu\nu}(k - p). \quad (7)$$

Here we have factorized the color factors in the effective interaction, $G_{\mu\nu}^{ab}(q) = \delta^{ab} G_{\mu\nu}(q)$ and performed the corresponding trace. The flavor content of the meson is not made explicit in eq. (7) as we have suppressed the flavor labels in the quark propagators. It is understood that the two propagators in eq. (7) are taken such as to account for the flavor quantum numbers of the considered meson. In the model that we will consider, the up and down quarks will be assumed to have equal current masses (m_0 in eq. (5)) and thus also identical propagator functions $A(x)$ and $B(x)$. For the light quarks, which should give rise to the familiar $SU(3)_f$ nonet, we are thus left with three representatives of each of the multiplets that are distinguished by their isospin number, $I = 0, \frac{1}{2}, 1$. We must also specify the meson angular momentum and parity. This is reflected by the Dirac and Lorentz decomposition of the meson vertex functions. This decomposition is known in the literature and here we follow Ref. [16]. For the pseudoscalar channel ($J^P = 0^-$) we take

$$\Gamma^{(P)}(p; P) = \gamma_5 \left[\Gamma_0^{(P)}(p; P) - i \not{P} \Gamma_1^{(P)}(p; P) - i \not{p} \Gamma_2^{(P)}(p; P) - [\not{P}, \not{p}] \Gamma_3^{(P)}(p; P) \right]. \quad (8)$$

The decomposition for a scalar ($J^P = 0^+$) meson reads

$$\Gamma^{(S)}(p; P) = \Gamma_0^{(S)}(p; P) - i \not{P} \Gamma_1^{(S)}(p; P) - i \not{p} \Gamma_2^{(S)}(p; P) - [\not{P}, \not{p}] \Gamma_3^{(S)}(p; P). \quad (9)$$

The vector ($J^P = 1^-$) channel involves eight scalar functions

$$\begin{aligned} \Gamma_\mu^{(V)}(p; P) = & \left[\gamma_\mu - \frac{P_\mu \not{P}}{P^2} \right] \left[i \Gamma_0^{(V)}(p; P) + \not{P} \Gamma_1^{(V)}(p; P) - \not{p} \Gamma_2^{(V)}(p; P) + i [\not{P}, \not{p}] \Gamma_3^{(V)}(p; P) \right] \\ & + \left[p_\mu - \frac{P_\mu p \cdot P}{P^2} \right] \left[\Gamma_2^{(V)}(p; P) + 2i \not{P} \Gamma_3^{(V)}(p; P) \right] \\ & + \left[p_\mu - \frac{P_\mu p \cdot P}{P^2} \right] \left[\Gamma_4^{(V)}(p; P) + i \not{P} \Gamma_5^{(V)}(p; P) - i \not{p} \Gamma_6^{(V)}(p; P) + [\not{P}, \not{p}] \Gamma_7^{(V)}(p; P) \right]. \end{aligned} \quad (10)$$

In the axialvector channel we have two modes that are distinguished by their charge conjugation properties [16]. For $J^{PC} = 1^{++}$ the decomposition is

$$\begin{aligned} \Gamma_{\mu}^{(A)}(p; P) = & \gamma_5 \left[\gamma_{\mu} - \frac{P_{\mu} \not{P}}{P^2} \right] \left[i\Gamma_0^{(A)}(p; P) + \not{P}\Gamma_1^{(A)}(p; P) - \not{p}\Gamma_2^{(A)}(p; P) + i[\not{P}, \not{p}]\Gamma_3^{(A)}(p; P) \right] \\ & + \gamma_5 \left[p_{\mu} - \frac{P_{\mu} p \cdot P}{P^2} \right] \left[\Gamma_2^{(A)}(p; P) + 2i\not{P}\Gamma_3^{(A)}(p; P) \right], \end{aligned} \quad (11)$$

while the $J^{PC} = 1^{+-}$ mode is decomposed as

$$\Gamma_{\mu}^{(\tilde{A})}(p; P) = \gamma_5 \left[p_{\mu} - \frac{P_{\mu} p \cdot P}{P^2} \right] \left[\Gamma_1^{(\tilde{A})}(p; P) + i\not{P}\Gamma_2^{(\tilde{A})}(p; P) - i\not{p}\Gamma_3^{(\tilde{A})}(p; P) + [\not{P}, \not{p}]\Gamma_4^{(\tilde{A})}(p; P) \right]. \quad (12)$$

In what follows we will omit the superscripts that label the spin and parity channels because these channels do not mix and there should hence be no confusion.

The primary object of this paper is to extract the bound state masses for the various flavor combinations and angular momentum channels.² The corresponding projection results in sets of coupled equations for the Γ_i . After carrying out two of the three angular integrals analytically we are left with functions of the squared momenta p^2 and P^2 as well as the angle between p and P : $z = p \cdot P / \sqrt{p^2 P^2}$. The z -dependence is analyzed by an expansion in Chebyshev polynomials T_k

$$\Gamma_i(p; P) = \sum_{k=0}^{N_{ch}-1} (i)^k \Gamma_i^k(p^2; P^2) T_k(z). \quad (13)$$

Since the T_k form an orthonormal set, we can project the equations for the Dirac components onto $\Gamma_i^k(p^2; P^2)$. Finally, the k^2 -integral in the Bethe–Salpeter equation (7) is implemented numerically as a matrix equation for the unknown $\Gamma_i^k(p_j^2; P^2)$, p_j^2 being the discrete values of the momentum squared. The kernel, K of that matrix parametrically depends on the meson momentum P^2 . We solve that matrix equation as an eigenvalue problem by tuning the meson momentum to $P^2 = -M^2$, such that $\text{Det}(1 - K) = 0$. This yields the desired meson mass M .

For practical reasons we need to truncate the expansion (13) at a certain order, N_{ch} . As noted before this violates relativistic covariance. Fortunately the momentum partition dependence provides a measure for the degree at which covariance is violated. We can mitigate this degree by increasing N_{ch} . Numerically we furthermore scan the momentum partition dependence of the computed meson masses to *a posteriori* verify covariance for our solutions to the Bethe–Salpeter equations, see Appendix A. Unless otherwise stated we use $N_{ch} = 4$.

² The traceology that is involved to project the Bethe–Salpeter equation (7) onto the Dirac components Γ_i is lengthy, but straightforwardly performed using the algebraic manipulation package FORM [17].

B. Pseudoscalar leptonic decay constant

The solution to the Bethe–Salpeter equation not only yields the meson masses but also the meson quark vertex functions that can be used to compute meson properties. Here we will focus on the pseudoscalar decay constants f_π and f_K . In order to calculate these, we first have to normalize the vertex functions $\Gamma(p; P)$. The Bethe–Salpeter equation is a homogeneous equation, and thus needs an additional normalization condition. As mentioned previously, that condition is obtained from demanding the pole in the four–quark Green’s function to be unity. For equal momentum partitioning, (*i.e.* for $\xi = 1/2$ only) it reads [15]

$$2P_\mu = 3 \int \bar{d}^4k \operatorname{Tr} \left\{ \bar{\Gamma}(k, -P) \frac{\partial S(k + P/2)}{\partial P_\mu} \Gamma(k, P) S(k - P/2) + \bar{\Gamma}(k, -P) S(k + P/2) \Gamma(k, P) \frac{\partial S(k - P/2)}{\partial P_\mu} \right\} \quad (14)$$

where the trace is over Dirac matrices. The conjugate vertex function $\bar{\Gamma}$ is defined as

$$\bar{\Gamma}(p, -P) = C \Gamma^T(-p, -P) C^{-1}, \quad (15)$$

where use is made of the charge conjugation matrix, $C = -\gamma_2 \gamma_4$. The quark propagator derivatives are calculated by differentiating the quark Schwinger–Dyson equations (4) and (5) analytically and then numerically integrating the corresponding expressions.

The decay constants are finally obtained from the coupling of the axial current to the quark loop [15]

$$f = \frac{3}{M^2} \int \bar{d}^4k \operatorname{Tr} \{ \Gamma(k, -P) S(k + P/2) \gamma_5 \not{P} S(k - P/2) \}, \quad (16)$$

where again the trace is over the Dirac matrices and the vertex functions are normalized according to eq. (14). Again we have not made explicit the flavor quantum numbers.

IV. NUMERICAL RESULTS AND DISCUSSION

We are now in the position to present our numerical results to the system of Schwinger–Dyson and Bethe–Salpeter equations. Even though the meson results are the primary target of our investigation it is fruitful to first consider the quark propagator functions obtained from the Schwinger–Dyson equations, as they enter the kernel of the Bethe–Salpeter equations.

A. Quark propagator functions

In Fig. 1 we show the quark propagator functions $A(p^2)$, $B(p^2)$ and $M(p^2) = B(p^2)/A(p^2)$ along the positive, real spacelike axis, $p^2 > 0$. This is the numerical solution to the coupled equations (6), which we emphasize is the basis for the quark solutions for complex momenta. The solution clearly shows that dynamical chiral symmetry breaking is occurring: the mass function $M(p^2)$ attains a sizable non–zero value, even in the case that the bare quark mass

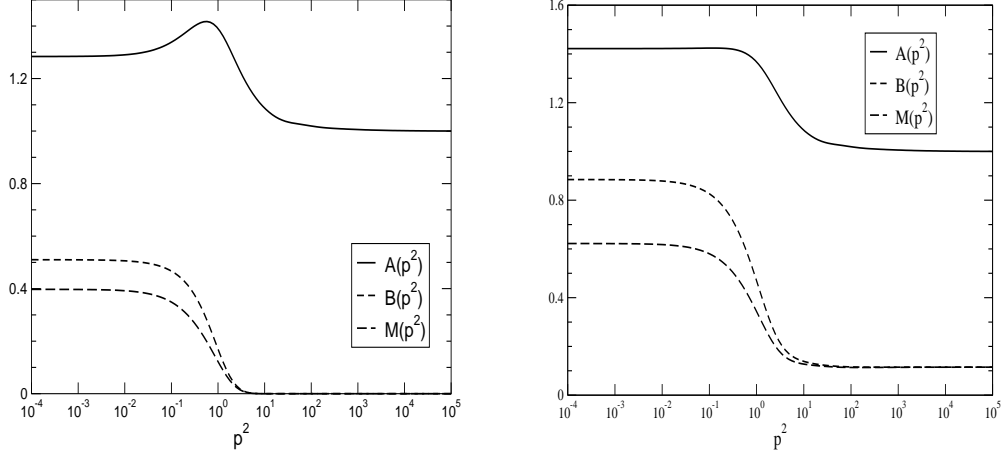


FIG. 1. Plot of the spacelike chiral quark functions (as a function of the momentum squared). The parameters are $\omega = 0.5\text{GeV}$, $D = 16.0\text{GeV}^{-2}$. Left panel: $m_0 = 0$, right panel: $m_0 = 0.115$ GeV. All units are GeV.

ω	D	m_0	$M(p^2 = 0)$
0.4	45.0	0	0.520
		5×10^{-3}	0.531
		0.12	0.709
0.45	25.0	0	0.450
		5×10^{-3}	0.462
		0.12	0.657
0.5	16.0	0	0.397
		5×10^{-3}	0.413
		0.115	0.622

TABLE I. The variation of the quark mass function evaluated at zero momentum squared. All units are GeV.

m_0 is zero. This phenomenon has been extensively studied (see for example Refs. [2,5]), and is an example of genuinely non-perturbative behavior as dynamical mass generation cannot occur at any order in perturbation theory. Recall that the effective interaction (1) that enters the Schwinger–Dyson equations does not contain the perturbative UV behavior, rather it has an exponential damping at high momenta. This is manifested in the quark propagator functions as a sharp transition from the low momentum behavior to the bare values in the high momentum region. This transition occurs at about 1GeV.

The quark mass function $M(p^2)$ is also a useful quantity to discuss the changes of the quark propagator with the input parameters. Table I shows $M(p^2 = 0)$ for those parameter sets of ω , D and m_0 that we will later use to compute the meson masses. As already mentioned the quark mass function indicates the extent to which dynamical chiral symmetry breaking occurs and plays the role of the mass of the constituent quarks within hadrons. We see that the quark mass function decreases as the effective scale ω increases and the

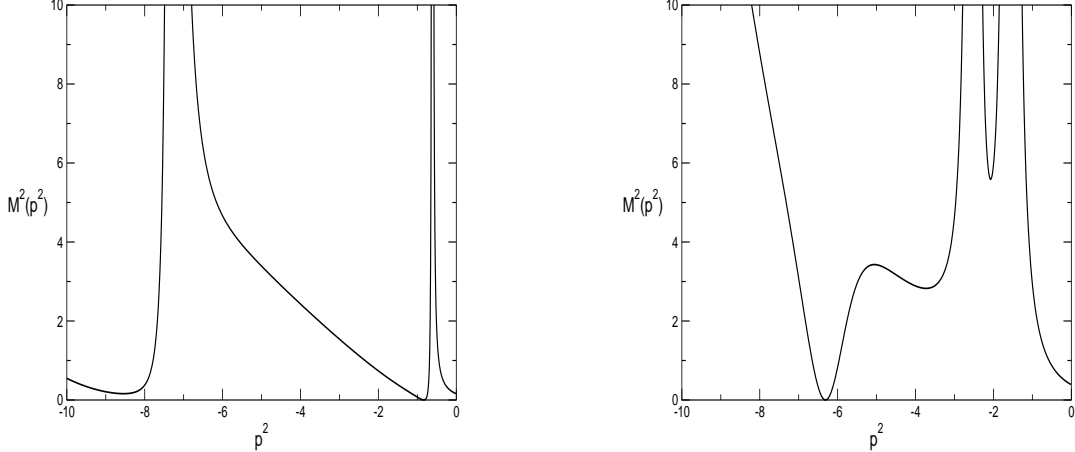


FIG. 2. Plot of the timelike quark mass function squared $M^2(p^2)$. The parameters are $\omega = 0.5, D = 16.0$. Left panel: $m_0 = 0$, right panel: $m_0 = 0.115$. All units are GeV.

strength D decreases.

Since the main thrust of the paper is the use of the quark propagator functions evaluated at precisely the complex momenta squared for which they enter the Bethe–Salpeter equation, it is important to study the behavior of the mass function at least along the timelike axis, *i.e.* for negative real momenta squared. In Fig. 2 we present typical results for the mass function squared $M^2(p^2)$ in that regime. Although the effective interaction (1) is simple, the timelike functions are distinctly non-trivial. Already from Fig. 2 we observe a significant variation with the current quark mass. This indicates that the specific forms of timelike quark propagator functions possess pronounced model and parameter dependences. Investigating the model dependence requires changing the effective interaction (1) and is not subject of the present study. For the parameter dependence, we fortunately find (see below) that it does not significantly effect the model predictions for the meson masses. There are divergences whenever A and B change sign at different p^2 . Note that there are several particle-like poles ($p^2 = -M^2(p^2)$) where the quark goes on-shell. This is an important observation, since it is not at all clear whether a confined quark can be on-shell. Indeed, one might be tempted to conclude that with on-shell singularities and a subsequent lack of confinement, the model will not be able to give meson masses at all. As we will see, this is fortunately not the case.

B. Mesons

Turning to the mesons, we note that there are four model parameters, ω, D, m_u and m_s that we first have to fit to empirical data. To this end, we initially choose the pseudoscalar meson observables M_π, M_K and f_π . Then one parameter remains unconstrained by the pseudoscalar sector alone. However, the condition that the quark propagator function reflects dynamical chiral symmetry breaking, *i.e.* that $M(p^2 = 0) \approx 0.5\text{GeV}$ leaves only a small window for the remaining choice, *cf.* table I. All other masses and decay constants are subsequently model predictions. The resulting model parameter and the predicted kaon decay constant f_K , that is unexpectedly well reproduced, are shown in Table II. The subsequently

ω	D	m_u	m_s	M_π	f_π	M_K	f_K
0.40	45.0	5×10^{-3}	0.120	0.135	0.131	0.496	0.164
0.45	25.0	5×10^{-3}	0.120	0.135	0.131	0.496	0.163
0.50	16.0	5×10^{-3}	0.115	0.137	0.133	0.492	0.164
experiment [18]				0.135	0.131	0.498	0.160

TABLE II. Parameter sets used and fit results for the pseudoscalar mesons. M_π , f_π and M_K are used as input, f_K is predicted. All units are GeV.

ω	D	m_u	m_s	M_ρ	M_{K^*}	M_ϕ
0.40	45.0	5×10^{-3}	0.120	0.748	0.939	1.072
0.45	25.0	5×10^{-3}	0.120	0.746	0.936	1.070
0.50	16.0	5×10^{-3}	0.115	0.758	0.946	1.078
experiment [18]				0.770	0.892	1.020

TABLE III. Results for the vector mesons. All units are GeV.

predicted meson masses are shown in Tables III-VI. In all cases we have the inequalities $M_{u\bar{u}} < M_{u\bar{s}} < M_{s\bar{s}}$, where the subscript labels the flavor content. These relations just reflect the quark–antiquark picture that is implicit in the present Bethe–Salpeter approach.

Obviously both the pseudoscalar (table II) and vector mesons (table III) can be very well described within our model with the choice $\omega \approx 0.5\text{GeV}$. Our results agree with a previous analysis of the vector mesons based on an effective interaction which included the perturbative type term [10]. This shows that such terms do not have a large effect on the meson masses, at least for the pseudoscalar and vector cases. Indeed, in the context of low–energy meson phenomenology we conclude that the logarithmic tail, and its associated renormalization represent an unnecessary obfuscation.

The situation for the scalar mesons (table IV) is not quite that clear. To begin with the particle data group [18] does not provide a clear picture in this channel but only quotes a wide range for the mass of the lowest scalar (0.4 – 1.2 GeV). More detailed studies of the pseudoscalar scattering amplitudes revealed that the assignment of the scalar meson nonet is not at all established [1]. In particular, these mesons may not be simple quark–antiquark bound states but *e.g.* might contain sizable admixture of 2quark–2antiquark pairs [14]. In that respect we might interpret our results as a quark–antiquark model prediction for scalar mesons. Our results suggest that such a picture is too simple for these mesons. One might also speculate that the adopted ladder approximation could be insufficient.

For the axialvector mesons we have two channels that are distinguished by their charge conjugation properties, *cf.* tables V and VI. The quark–antiquark pairs that are bound to axialvector modes with negative charge conjugation eigenvalue tend to be lighter than those with the positive eigenvalue but otherwise equal quantum numbers. Generally we find that our predictions are lower than the assignments made by the particle data group [18].

We recognize from our results that the model predictions change only slightly within the

ω	D	m_u	m_s	$M_{u\bar{u}}$	$M_{u\bar{s}}$	$M_{s\bar{s}}$
0.40	45.0	5×10^{-3}	0.120	0.700	0.917	1.096
0.45	25.0	5×10^{-3}	0.120	0.675	0.908	1.099
0.50	16.0	5×10^{-3}	0.115	0.645	0.903	1.113

TABLE IV. Results for the scalar mesons. The subscripts of M denote the flavor content. All units are GeV.

ω	D	m_u	m_s	$M_{u\bar{u}}$	$M_{u\bar{s}}$	$M_{s\bar{s}}$
0.40	45.0	5×10^{-3}	0.120	0.804	0.994	1.128
0.45	25.0	5×10^{-3}	0.120	0.858	1.047	1.182
0.50	16.0	5×10^{-3}	0.115	0.912	1.098	1.230
experiment [18]				1.230	1.270	1.170 ?

TABLE V. Results for the axial-vector ($J^{PC} = 1^{+-}$) mesons. The question mark indicates that the PDG did not assign the charge conjugation property of the respective resonance. All units are GeV.

ω	D	m_u	m_s	$M_{u\bar{u}}$	$M_{u\bar{s}}$	$M_{s\bar{s}}$
0.40	45.0	5×10^{-3}	0.120	0.917	1.117	1.253
0.45	25.0	5×10^{-3}	0.120	0.918	1.124	1.270
0.50	16.0	5×10^{-3}	0.115	0.927	1.140	1.292
experiment [18]				1.230	1.270	1.282

TABLE VI. Results for the axial-vector ($J^{PC} = 1^{++}$) mesons. All units are GeV.

ω	D	m_u	m_s	$M_{u\bar{u}}$	$M_{u\bar{s}}$	$M_{s\bar{s}}$
0.40	45.0	5×10^{-3}	0.120	0.807	0.990	1.131
0.45	25.0	5×10^{-3}	0.120	0.861	1.040	1.185
0.50	16.0	5×10^{-3}	0.115	0.915	1.085	1.233

TABLE VII. Results for the axial-vector mesons allowing for mixing of the Dirac structures in eqs. (11) and (12). All units are GeV.

large range of considered model parameters. This confirms that meson static properties are not too sensitive to the conjectural parameter dependence of the timelike quark propagator functions. Presumably meson properties whose computation involves larger timelike will exhibit a stronger sensitivity.

Already from table V we observe that by increasing ω the predicted mass of the $J^{PC} = 1^{+-}$ meson with pion flavor quantum numbers approaches the empirical mass³. We therefore further increased ω according to the rules discussed above. For $\omega \sim 0.8\text{GeV}$ we reproduced the empirical value for the mass in that channel. However, this happened at the expense of significantly lowering f_K and loosing the proper description of the vector mesons. We recall that the parameter ω has a physical interpretation as the location of the maximum of the interaction. Thus $\omega = 0.8\text{GeV}$ seems intuitively too large for low-energy hadron physics and an unsatisfactorily description of the 0^- and 1^- mesons comes without surprise.

For non-diagonal flavor structures such as $u\bar{s}$, charge conjugation actually is not a sensible quantum number and the corresponding axial vector mesons 1^{++} and 1^{+-} may mix. In table VII we present the results obtained from the full calculation that combines the Dirac decompositions (11) and (12). Since our Bethe-Salpeter formalism only yields the lowest mass eigenstate within a given channel, the results presented in table VII should be compared to those in table V. The tiny changes for the flavor diagonal mesons are numerical artifacts. Surprisingly the changes for the non-diagonal flavor structure are also only of the order 1%. This suggests only a small mixing between the 1^{++} and 1^{+-} states with the flavor structure $u\bar{s}$ and the 1^{++} and 1^{+-} channels represent good approximations to the actual eigenstates.

We can extend our model beyond the light flavors up, down and strange. The only modification is the increase of the current quark mass, m_0 . In Fig. 3 we show how the meson masses increase as the (equal) quark masses are increased into the charm sector $m_c = 1.125\text{GeV}$. Exactly the same numerical code is used to construct these solutions to the Schwinger-Dyson and Bethe-Salpeter equations as for the light flavors. Clearly seen is the smooth way the masses increase from the chiral limit ($m_0 = 0$) into the heavy quark sector ($m_0 = m_c$). This represents a convincing indicator for the stability of our technique. The $c\bar{c}$ -meson masses can be loosely extracted (table VIII) and the data are surprisingly well reproduced. We did not expect to be able to describe such a heavy system with such a simple model, derived (and fitted) as it is from pion physics. The lack of the correct UV

³In all other channels the dependence on the parameters is much softer within the allowed window.

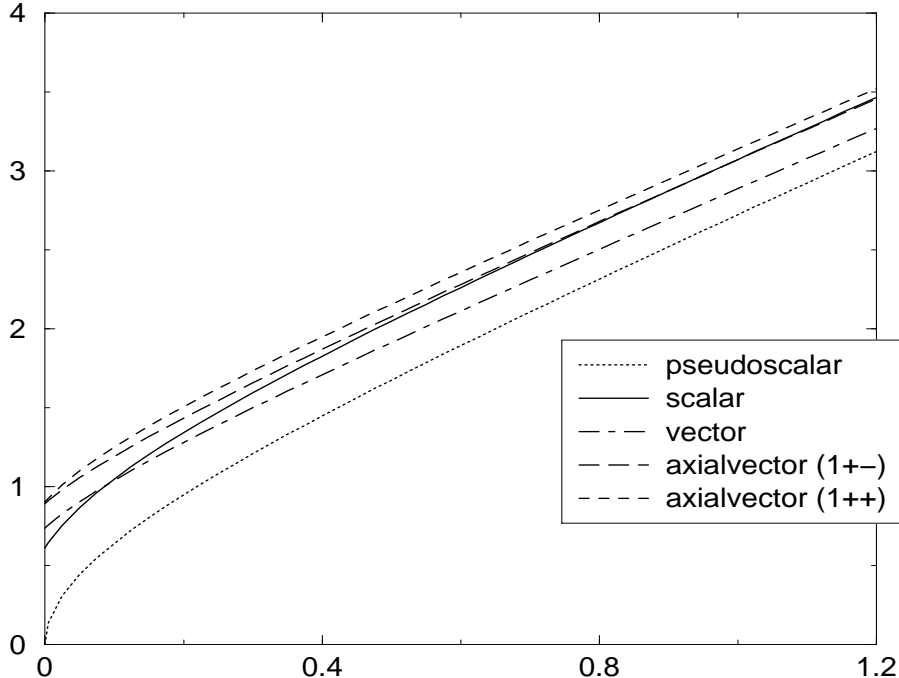


FIG. 3. Meson masses as a function of the (equal) quark mass, m_0 . $\omega = 0.5\text{GeV}$, $D = 16\text{GeV}^{-2}$. All units are GeV.

$J^{P(C)}$	$M_{c\bar{c}}$	experiment [18]
0^-	2.97	η_c : 2.98
1^-	3.13	J/ψ : 3.10
0^+	3.32	χ_{c0} : 3.42
1^{++}	3.38	χ_{c1} : 3.51
1^{+-}	3.31	?

TABLE VIII. Results for the $c\bar{c}$ -meson states. $\omega = 0.4$, $D = 45.0$, $m_c = 1.125$. m_c is fitted approximately from the η_c mass.

behavior for the gluon is seemingly at odds with the scales present. However, the present results suggest that the Bethe–Salpeter equation is capable of describing *all* the angular momentum states equally well in the charm quark sector.

V. SUMMARY AND OUTLOOK

In this paper we have studied the low-lying mesons as quark–antiquark bound states in a covariant approach using an effective interaction. This interaction is characterized by gluon exchange with the gluon propagator being dressed by a Gaussian shape function. The interaction is completed by the quark–gluon vertex that we take to be the tree-level perturbative one. In this manner the rainbow–ladder approximation to the system of Schwinger–Dyson and Bethe–Salpeter equation accounts for chiral symmetry. With this

effective interaction, we have then consistently treated this system of integral equations by precisely implementing the quark propagator functions that solve the Schwinger–Dyson equations into the Bethe–Salpeter equations. Once the effective interaction exceeds a certain strength, the Schwinger–Dyson equations exhibit dynamical chiral symmetry breaking and the pseudoscalar mesons emerge as *would-be* Goldstone bosons. We have then used observed properties of the pseudoscalar mesons to determine the model parameters. The kaon decay constant represents a model prediction. It turned out to be in good agreement with the empirical data. Furthermore our results for the vector meson masses match the experimental data. The situation in the scalar channel is less satisfying. As we solely consider the mesons as bound states of quark–antiquark pairs, it is not surprising that the mass eigenvalues increase with the strangeness content. On the other hand it is astonishing that for current quark masses, $m_0 \geq 0.2\text{GeV}$, the lightest scalar mesons turn out to be heavier than the lightest vector mesons. When discussing these results it must be noted that the role of the scalar mesons is still under intense debate. In particular, the question whether they should indeed be considered as quark–antiquark bound states is not yet completely resolved. There are indications, see e.g. Ref. [1] and references therein, that the scalar meson masses should actually decrease with the strangeness content of these mesons. This can be understood if these mesons are considered as 2quark–2antiquark bound states in the sense of diquark–antidiquark systems [14].

As an outlook we mention that there is an elegant way to extend the present model to incorporate such degrees of freedom. The Bethe–Salpeter treatment can be straightforwardly extended to study bound states of diquark–antidiquark pairs, once a binding mechanism is established. This could either be achieved by a gluon exchange similar to eq. (1) or by quark exchange between a quark and a diquark. The latter approach has been intensively studied and the corresponding vertex is known from modeling baryon properties [19]. It will also be interesting to see whether these additional degrees of freedom will also affect the mass predictions for the axialvector mesons that currently tend to be on the low side. Investigations in this direction are in progress.

Finally we would like to repeat that the stability of our treatment – measured by the actual momentum partition invariance – allows us to even describe mesons with charm quantum numbers. Without further modifications of the model parameter, except the corresponding current quark mass, our approach reproduces the mass eigenvalues of the flavor neutral states unexpectedly well.

ACKNOWLEDGMENTS

We thank J.C.R. Bloch, C. S. Fischer, D. J. Länge, P. Maris, M. Oettel, H. Reinhardt, S. M. Schmidt, and P. C. Tandy for valuable discussions. This work has been supported by DFG (Al-297/3-3, Al-297/3-4, We-1254/3-2, We-1254/4-2) and COSY (contract no. 41376610).

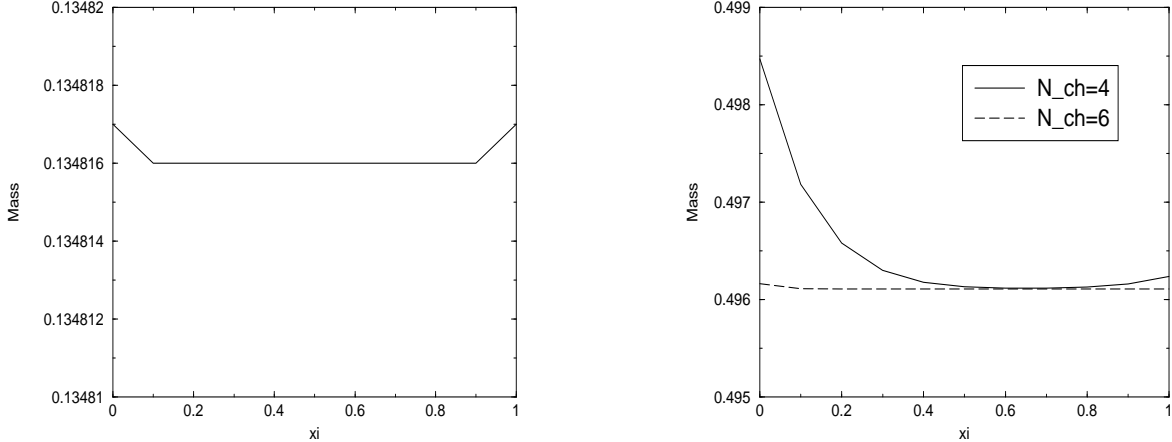


FIG. 4. Dependence of the pion (left) and kaon (right) masses on the momentum partition ξ . Model parameters are: $\omega = 0.4$, $D = 45$, $m_u = 5 \times 10^{-3}$ and $m_s = 0.120$. All units are GeV. For the calculation of the pion mass $N_{\text{ch}} = 4$ has been used.

APPENDIX A: RELATIVISTIC COVARIANCE

As mentioned in section III the truncation of taking N_{ch} finite in eq. (13) violates relativistic covariance. Studying the dependence of our results on the momentum partitioning parameter ξ we can provide a measure of these violations originating from the numerical method. The results for the pseudoscalar case are shown in Fig. 4. The pion mass is extremely stable over the whole range $\xi \in [0, 1]$, whereas for the kaon, the asymmetry between the quark masses must be compensated for by increasing the number of Chebyshev moments, N_{ch} . Clearly, for the light pseudoscalars, the technique of inserting the quark propagators directly results in extremely stable results. In the case of the other mesons, the stability becomes less evident as one is studying heavier mass resonances (but with the same quarks). As an example, we display the axial-vector ($J^{PC} = 1^{+-}$) $u\bar{s}$ meson (Fig. 5). There is still a clear range of stability $\xi \in [0.4, 0.7]$. Outside this range however, we notice that the technique does not simply break down (a mass can still be found) – it merely gets numerically more difficult to get trustworthy results. We assert the increasing dependence on ξ with larger meson masses to the fact that with larger meson masses the calculation becomes more sensitive to the violent behavior seen in the timelike quark propagator functions. The larger the influence of that behavior to the calculation the higher we have to assume the number of Chebyshev moments for an adequate representation. Away from this timelike regime the quark propagator functions are smooth. This results in a good representation of the Bethe–Salpeter kernel and vertex functions with only a few Chebyshev moments.

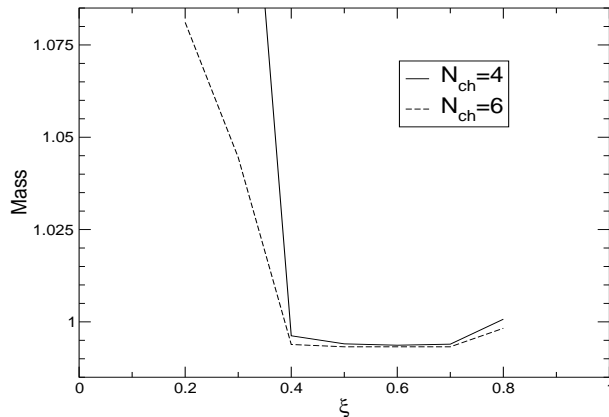


FIG. 5. Dependence of the axial-vector ($J^{PC} = 1^{+-}$) mass on the momentum partition ξ . One set of parameters has been used: $\omega = 0.4$, $D = 45$, $m_u = 5 \times 10^{-3}$ and $m_s = 0.120$. All units are GeV.

REFERENCES

- [1] D. Black *et al.*, Phys. Rev. **D64** (2001) 014031, [arXiv:hep-ph/0012278].
N. A. Törnquist, hep-ph/0201171: *The Lightest Scalar Nonet*; M. Ishida, hep-ph/9905259: *Existence of $\sigma(600)/\kappa(900)$ and possible classification of chiral scalar nonet*; N. N. Achasov, hep-ph/0201299: *Radiative decays of ϕ -meson and nature of light scalar resonances*.
- [2] R. Alkofer and L. von Smekal, Phys. Rept. **353** (2001) 281, [arXiv:hep-ph/0007355].
- [3] J. E. Mandula, Phys. Rept. **315** (1999) 273; F. D. Bonnet, P. O. Bowman, D. B. Leinweber and A. G. Williams, Phys. Rev. **D62** (2000) 051501 [arXiv:hep-lat/0002020]; F. D. Bonnet, P. O. Bowman, D. B. Leinweber, A. G. Williams and J. M. Zanotti, Phys. Rev. **D64**, (2001) 034501, [arXiv:hep-lat/0101013]; K. Langfeld, H. Reinhardt and J. Gattnar, Nucl. Phys. **B621** (2002) 131, [arXiv:hep-ph/0107141].
- [4] L. von Smekal, R. Alkofer and A. Hauck, Phys. Rev. Lett. **79** (1997) 3591, [arXiv:hep-ph/9705242]; Annals Phys. **267** (1998) 1, [arXiv:hep-ph/9707327].
- [5] C. D. Roberts and S. M. Schmidt, Prog. Part. Nucl. Phys. **45** (2000) S1, [arXiv:nucl-th/0005064].
- [6] Y. Nambu and G. Jona-Lasinio, Phys. Rev. **122** (1961) 345; **124** (1961) 246.
- [7] D. Ebert and H. Reinhardt, Nucl. Phys. **B271** (1986) 188.
- [8] P. Jain and H. J. Munczek, Phys. Rev. **D48** (1993) 5403, [arXiv:hep-ph/9307221]; G. Krein, C. D. Roberts and A. G. Williams, Int. J. Mod. Phys. A **7** (1992) 5607.
- [9] P. Maris, C. D. Roberts and P. C. Tandy, Phys. Lett. **B420** (1998) 267, [arXiv:nucl-th/9707003].
- [10] P. Maris, and P.C. Tandy, Phys. Rev. **C60** (1999) 055214, [arXiv:nucl-th/9905056].
- [11] C. D. Roberts, Nucl. Phys. **A605** (1996) 475, [arXiv:hep-ph/9408233].
- [12] P. Maris and C. D. Roberts, Phys. Rev. **C56** (1997) 3369, [arXiv:nucl-th/9708029].
- [13] A. Bender, C. D. Roberts and L. von Smekal, Phys. Lett. **B380** (1996) 7, [arXiv:nucl-th/9602012]; G. Hellstern, R. Alkofer and H. Reinhardt, Nucl. Phys. **A625** (1997) 697, [arXiv:hep-ph/9706551];
- [14] R. L. Jaffe, Phys. Rev. **D15** (1977) 267.

- [15] P.C. Tandy, Prog. Part. Nucl. Phys **39** (1997) 117, [arXiv:nucl-th/9705018].
- [16] C.H. Llewellyn-Smith, Ann. Phys **53** (1953) 521.
- [17] J.A.M. Vermaseren, math-ph/0010025: *New Features of FORM*.
- [18] D.E. Groom *et al.* (Particle Data Group), Eur. Phys. J. **C15**, (2000) 1, and 2001 partial update for edition 2002 (URL: <http://pdg.lbl.gov>).
- [19] M. Oettel, G. Hellstern, R. Alkofer and H. Reinhardt, Phys. Rev. **C58** (1998) 2459, [arXiv:nucl-th/9805054]; M. Oettel, M. Pichowsky and L. v. Smekal, Eur. Phys. J. **A8** (2000) 251, [arXiv:nucl-th/9909082]; M. Oettel, R. Alkofer and L. von Smekal, Eur. Phys. J. **A8** (2000) 553, [arXiv:nucl-th/0006082]; S. Ahlig *et al.*, Phys. Rev. **D64** (2001) 014004, [arXiv:hep-ph/0012282].